Case History of a Geosynthetic-Stabilized Base Roadway Founded over Expansive Clay Subgrade

L. Zheng[1]; G. H. Roodi, Ph.D.[2]; and J. G. Zornberg, Ph.D., P.E.[3]

[1]Dept. of Civil, Architectural, and Environmental Engineering, Univ. of Texas at Austin, 301 E. Dean Keeton St., Stop C1792, Austin, TX 78712
[2]Dept. of Civil, Architectural, and Environmental Engineering, Univ. of Texas at Austin, 301 E. Dean Keeton St., Stop C1792, Austin, TX 78712
[3]Dept. of Civil, Architectural, and Environmental Engineering, Univ. of Texas at Austin, 301 E. Dean Keeton St., Stop C1792, Austin, TX 78712

ABSTRACT

Performance of a geosynthetic-stabilized base roadway founded over an expansive clay subgrade in Texas was evaluated over a period of 4 years. The construction involved three test sections. Two test sections were stabilized using two triangular geogrids of different characteristics and one test section was constructed without geogrid (control section). The geogrid layer was installed between a chemically-treated subbase and a flexible base layer. A comprehensive monitoring program was conducted to evaluate the performance of the roadway under environmental loads. Specifically, vertical movement of the roadway over time induced by recurring heave and settlement of the expansive clay subgrade was monitored. In addition, severity and extent of the environmental longitudinal cracks, identified as the main damage results from the expansive clay subgrade, were documented in each test section using data collected through rigorous visual condition surveys. Environmental conditions of the site, in form of changes in temperature and precipitation, was also closely monitored. Evaluation of the data collected on this roadway provided evidence for mechanisms that result in the development of environmental longitudinal cracks. In addition, comparison of the performance of the geogrid-stabilized test sections with the control section underscored the benefits from geosynthetic stabilization in mitigation of damages induced by the expansive clay subgrade. Furthermore, the observed difference between the performances of the two test sections stabilized with geogrids of different characteristics underscored the impact of geosynthetic characteristics on the benefits result from geosynthetic stabilization.

INTRODUCTION

Expansive clay subgrades have been reported as one of the major sources for damages to Texas roadways (Dessouky et al. 2012). The predominant form of damage to the roadways founded on expansive clay subgrades includes longitudinal cracks. These cracks are triggered by environmental changes that in turn result heave and settlement of the expansive clay subgrade. Therefore, they are often referred to as the environmental longitudinal cracks. A relevant mechanism that explains the development of the environmental longitudinal cracks has been detailed in previous publications by Zornberg et al. (2012) and Roodi et al. (2016). According to this mechanism, recurring wet and dry seasons result substantial changes in the moisture content of the expansive clay subgrade on the edges of the road while the moisture content in the subgrade located underneath the center of the road remains comparatively unchanged. Substantial difference between changes in the moisture content of the expansive clay subgrade on the edge and underneath the center of the road results differential vertical movement in the

road structure in which the edges heave (during wet seasons) and settle (during dry seasons) while the center remains comparatively stationary.

The Texas Department of Transportation (TxDOT) has adopted geosynthetic stabilization of the base course to mitigate detrimental impacts from expansive clay subgrades (Chen 2007). The efficiency of this technique has often been evaluated by studying the extent of environmental longitudinal cracks on roadways that were constructed with and without geosynthetic stabilization. This paper elaborates the case history of Cabeza Road founded on an expansive clay subgrade in Dewitt County, Texas. Two sections of this road were reconstructed using two triangular geogrids of different characteristics while a third section was reconstructed without geosynthetic. A comprehensive monitoring program was conducted to evaluate the mechanism resulting the development of environmental longitudinal cracks and to compare the performance of geosynthetic-stabilized sections with the performance of the control section.

PROJECT LOCATION

Cabeza Road, located in Dewitt County, Texas, is about 114 miles south of Austin, 84 miles east of San Antonio and 174 miles west of Houston (Figure 1). This road is a county road (Dewitt county road 324) connecting Ckodre road (Dewitt county road 352) and Texas State Highway 72 with a total length of 8.93 miles (Figure 2). The test sections are located approximately in the middle of this roadway along North-South direction as marked in Figure 2. The total length of the test sections are approximately 910 ft.

Figure 1. Location of Cabeza Road.

SECTION DESIGN

The test sections of Cabeza road were constructed in 2014. Three different designs were adopted including a 246-ft-long section stabilized using triangular geogrid GS1 (Section 1), a 246-ft-long control section without geosynthetic stabilization (Section 2), and a 417-ft-long section stabilized using triangular geogrid GS2 (Section 3) (Figure 3). A gas facility is located at the north side of Section 1 that may cause a comparatively higher traffic volume near its entrance. However, as part of a county road with asphalt chip seal surface, the test sections have had comparatively low traffic volumes. Based on traffic observations during multiple site visits, on average less than 10 vehicles were passed by this area within two hours in the middle of a day. The road design consisted of an asphalt chip seal at the surface supported with 6 in. of

flexible base layer, underlain by 6 to 8 in. of cement-stabilized subbase. The geosynthetic layer was placed at the interface of the base course and subbase. General design profiles are shown in Figure 4.

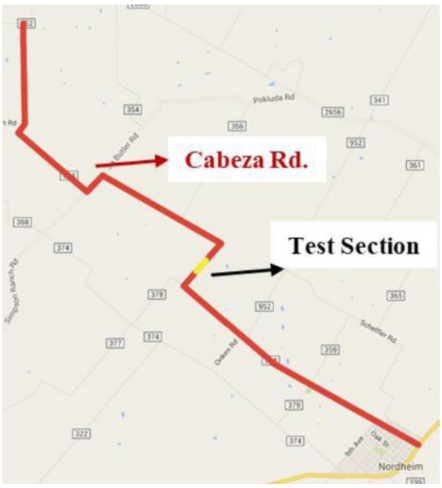

Figure 2. Location of test section along Cabeza Road.

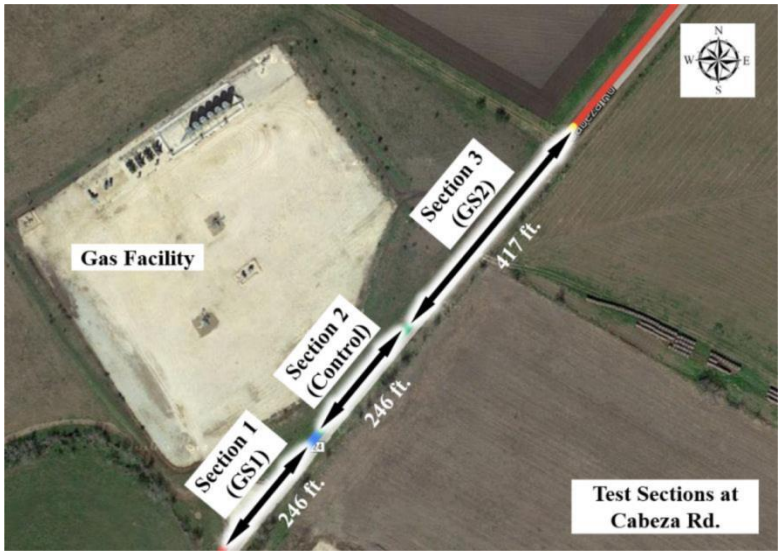

Figure 3. Layout of test sections.

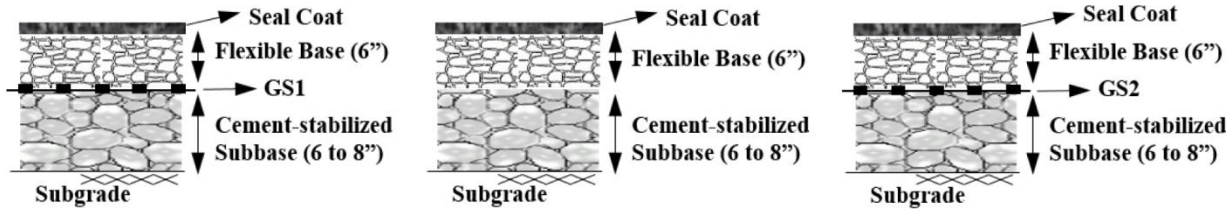

a) **b)** **c)**

Figure 4. Design profiles of test sections: a) Section 1 (stabilized using GS1); b) Section 2 (Control Section); c) Section 3 (stabilized using GS2).

MATERIAL PROPERTIES

Geosynthetics: Table 1 shows characteristics of the two triangular geogrids used in the test sections according to the manufacturer product specification sheets. GS2 has larger rib pitch (i.e., larger aperture size) than GS1. GS1 has larger mid-rib depth for diagonal ribs than GS2. The mid-rib depth for transverse ribs is the same for both geogrids. However, GS2 has larger mid-rib width than GS1 for both diagonal and transverse ribs. According to the manufacturer, GS2 is expected to provide a comparatively higher level of performance than GS1.

Table 1. Characteristics of geogrids

Index Properties	GS1	GS2
Rib Pitch, mm (in)	33 (1.30)	40 (1.60)
Diagonal Mid-rib depth, mm (in)	1.5 (0.06)	1.3 (0.05)
Diagonal Mid-rib width, mm (in)	0.6 (0.02)	0.9 (0.04)
Transverse Mid-rib depth, mm (in)	1.2 (0.05)	1.2 (0.05)
Transverse Mid-rib width, mm (in)	0.7 (0.03)	1.2 (0.05)
Radial stiffness at 0.5% strain, kN/m (lb/ft)	200 (13,700)	-

Subgrade soil: The soil map of test area was obtained from U.S. Department of Agriculture (USDA 2018) Web Soil Survey as shown in Figure 5. Based on the soil survey data reported by USDA for the region around Cabeza Road, the general soil type near the south part of Section 1 is Runge fine sandy loam (RuB) with 1 to 3 percent slopes. The overall soil type for the other parts of the test sections, including Sections 2 and 3 and the north part of Section 1, is Mabank fine sandy loam (MaA) with 0 to 1 percent slopes. Detailed soil properties of these two soil zones are listed in Table 2.

Figure 5: USDA Web Soil Survey soil map.

PERFORMANCE EVALUATION PROGRAM

Visual Condition Survey: As part of the field monitoring procedure in this project, condition surveys were conducted along each bound to evaluate extent and severity of environmental longitudinal cracks along the three test sections at Cabeza road. The percentage of

longitudinal cracks was calculated by the ratio of longitudinal crack length to the entire length of each section. Example results obtained from the latest condition survey conducted in May 2018 are presented in Figure 6. The best performance among the three test sections was observed in Section 3, which was stabilized using GS2 that had comparatively larger rib thickness than GS1 used in Section 1. Control section, which was not stabilized with geogrid, showed highest percentage of longitudinal cracks and a poor performance. Example pictures of longitudinal cracks observed in the control section are shown in Figure 7.

Table 2. Soil properties of Mabank fine sandy loam and Runge fine sandy loam

Map unit symbol	Depth	USDA texture	Classification		Passing sieve number				LL	PI
-	in	-	Unified	AASHTO	4	10	40	200	L-R-H	L-R-H
MaA-Mabank fine sandy loam, 0 to 1 percent slopes	0-7	Fine sandy loam	CL, CL-ML, SC, SC-SM	A-4, A-6	98	98	89	55	19-26-32	4-10-15
	7-56	Clay, clay loam	CH, CL	A-6, A-7	98	98	98	73	38-47-55	22-30-37
	56-84	Sandy clay loam, clay, clay loam	CH, CL	A-6, A-7	98	98	98	73	38-47-55	22-30-37
RuB-Runge fine sandy loam, 1 to 3 percent slopes	0-12	Fine sandy loam	SM, CL, SC, SC-SM	A-2-4, A-4	100	100	92	35	15-23-30	2-6-10
	12-44	Fine sandy loam, sandy clay loam, clay loam	SC, CL	A-7-6, A-6	99	98	96	48	30-35-46	11-17-25
	44-80	Fine sandy loam, sandy clay loam, loam	CL, SC, SM, SC-SM	A-7-6, A-2-4, A-4, A-6	89	87	81	38	15-22-41	2-9-20

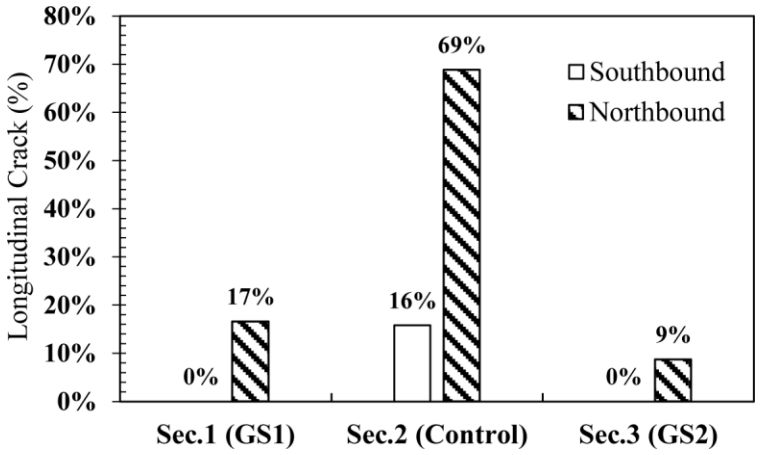

Figure 6. Percentage of longitudinal cracks at Cabeza Road test sections.

Total station survey: Vertical movement of the road surface over time was monitored using total station instrument using the procedure developed by Roodi et al. (2016). A total of five transverse sections were marked along Cabeza road test sections (Figure 8). One transverse section was marked in Section 1 (TS5) whereas two transverse sections were marked in Sections

2 (TS3 and TS4) and 3 (TS1 and TS2). Figure 9 presents an example of the marked transverse section located in test Section 2. The vertical movement of the marked sections was monitored using total station. A total of eleven total station surveys were conducted between 2015 and 2018. The first total station survey was conducted on August 31, 2015 and the last survey was conducted on May 9, 2018.

Figure 7. Example pictures of longitudinal cracks in Section 1 (Control).

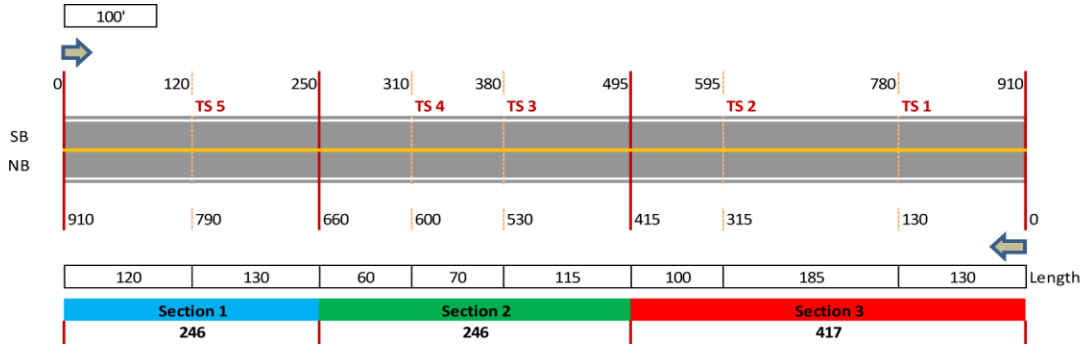

Figure 8. Sketch of transverse sections at Cabeza Road.

Figure 9. Transverse Section 3 (TS3) located in Control section.

Total station data was used to generate transverse section of the road at each marked section. Example plot of the transverse section for marked section 1 (TS1) is shown in Figure 10. The horizontal axis shows the distance from the centerline of the road while the vertical axis

corresponds to the relative elevation of each point compared to the elevation of the centerline. Negative values on the horizontal axis corresponds the south bound, while positive values on the horizontal axis correspond to the north bound. Assuming the elevation of the center point on the road remains unchanged (and equal to zero), transverse section profiles that were generated over time were superimposed in one plot. This presentation of data allowed evaluating differential movements between the center and the edges of the road over time.

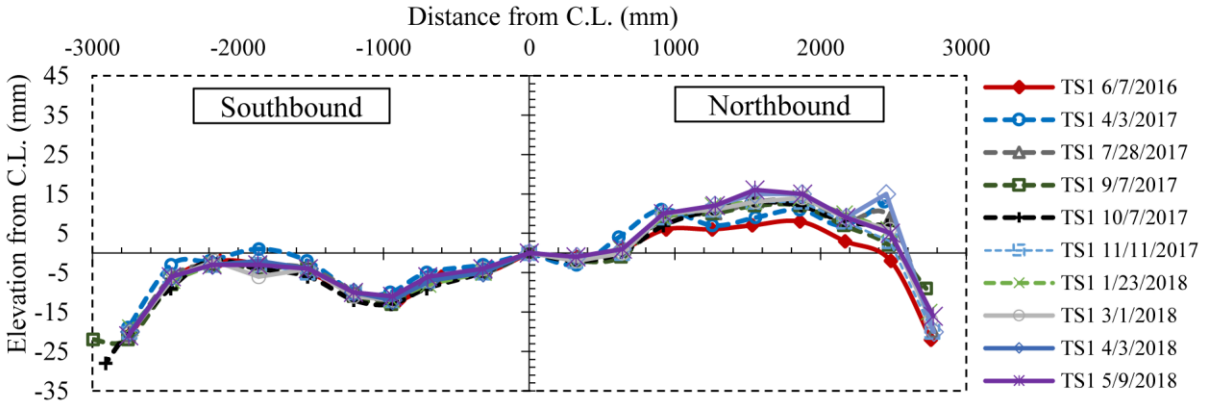

Figure 10. Example of changes in transverse profile of road over time.

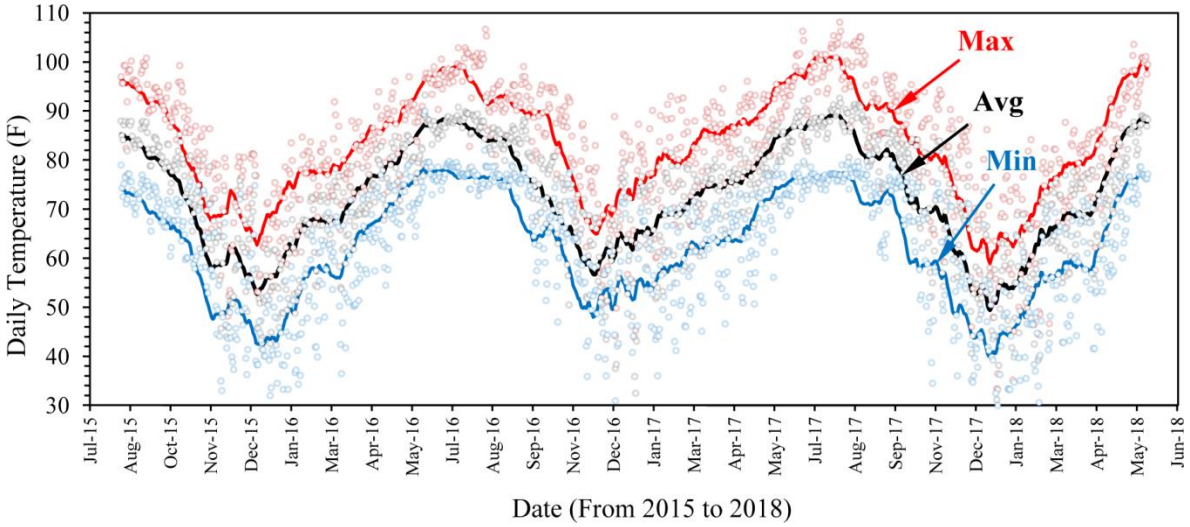

Figure 11. Daily temperature data from North Runge CR319 station.

Environmental data: In order to evaluate the influence of seasonal changes on the longitudinal cracks and shoulder movements, precipitation and temperature data was collected. This data was expected to be the most relevant data to swelling and shrinkage of the expansive clay subgrade. Precipitation and temperature data was collected from Weather Underground website (Weather Underground 2018). The closest radar station to the tests sections on Cabeza Road was found to be the North Runge CR319 (KTXRUNGE3).

Figures 11 and 12 present temperature and precipitation data collected from North Runge CR319 station. The horizontal axis of both graphs correspond to months from August 2015 to May 2018. The vertical axis corresponds to the daily temperature (in Fahrenheit) in Figure 11 and daily precipitation (in inches) in Figure 12. Evaluation of the temperature data presented in Figure 11 indicates that the roadway did not experience extreme hot or cold seasons and had

regular cycles of hot and cold climates repeated over the past three years.

Evaluation of the precipitation data presented in Figure 12 shows that in general, the test sections have experienced regular cycles of dry and wet seasons. The road experienced a seasonal raining period from May to September. The highest monthly rain was recorded in August 2016.

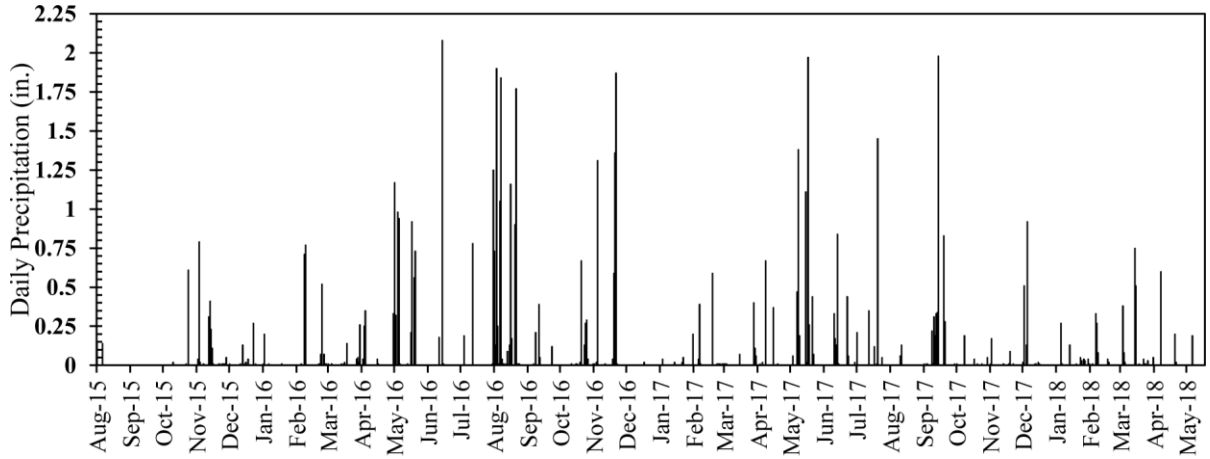

Figure 12. Daily precipitation data from North Runge CR319 station.

DISCUSSION OF RESULTS

Performance of Cabeza Road under environmental loads is discussed in this section by evaluating development of the longitudinal cracks over time along with variation in the elevation of the road surface and changes in the environmental conditions of the site.

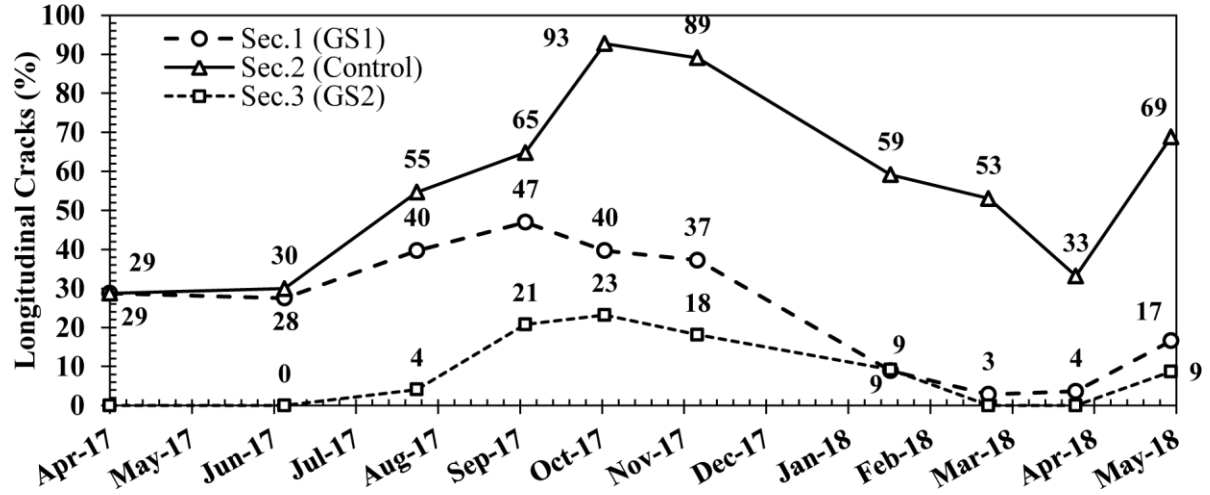

Figure 13. Percentage of longitudinal cracks over time in the northbound of test sections.

Development of environmental longitudinal cracks over time: Figure 13 shows changes in the percentage of environmental longitudinal cracks (on the vertical axis) over time (on the horizontal axis) for the three experimental test sections. Evaluation of the data in this figure indicates that the percentage of environmental longitudinal cracks were significantly higher in the control section than in the geosynthetic-stabilized sections. In addition, the test section stabilized using GS2 (Section 3) has continuously shown less cracks than the section stabilized

using GS1 (Section 1). This observation was consistent with the initial expectation because GS2 was expected to provide a better soil-geosynthetic interaction performance as compared to GS1 (Roodi et al. 2018).

Figure 14. Example pictures of opening and closing of cracks over time.

An additional observation in Figure 13 is that the percentage of cracks in all test sections increases and decreases over specific periods. Example pictures of opening and closing a longitudinal crack in different seasons are presented in Figure 14. To investigate potential reasons for this observation, in the subsequent sections periodical changes in the percentage of longitudinal cracks were compared to the vertical movements of the road surface and the environmental data.

Correlation between development of environmental longitudinal cracks and vertical movement of road surface: The elevation data obtained in total station measurements of transverse sections was used to present the relative elevation of the road surface compared to the elevation recorded in the first visit (Figure 15). Specifically, the elevations of cross section points in the first visit were subtracted from the elevations in the subsequent visits. Therefore, the cross section profile corresponded to the first visit are represented by a flat line in Figure 15. This presentation provided a clearer demonstration for pavement vertical movements over time. The

right sides of the plots in Figure 15 (i.e., distance from C.L. > 0) show relative elevation of the road surface on the northbound and the left sides (i.e., distance from C.L. < 0) represent the data for the southbound.

Comparatively more fluctuations in the elevations presented on the right side of plots (i.e., northbound) were observed than those on the left side (i.e., southbound). The data obtained in the condition surveys were also showed that northbound had comparatively larger percentage of environmental longitudinal cracks than the southbound (Figure 6). Except for a small amount of cracks in the control section, no crack was developed in the southbound of the test sections and almost all cracks were developed along the northbound. This observation suggests a correlation between fluctuations in the elevation of the road and the development of the environmental longitudinal cracks. That is higher fluctuations in the elevation of road surface may result larger percentage of environmental longitudinal cracks.

Comparing the vertical movements of the northbound lanes between the control section (i.e., TS3 and TS4 presented in Figures 15c and d) and the geosynthetic-stabilized sections (i.e., TS1, TS2, and TS5 presented in Figures 15a, b, and e) highlights the influence of geosynthetic. Although geosynthetic stabilization did not result a reduced vertical movement of the road, it mitigated the development of environmental longitudinal cracks. Specifically, for the same (or even larger) amount of vertical movements observed for the northbound of the geosynthetic-stabilized sections (i.e., TS1, TS2, and TS5) as that in the control section (i.e., TS3 and TS4), the percentage of environmental longitudinal cracks was significantly lower in the stabilized sections.

Furthermore, evaluation of the data presented in Figure 15 along with the dates corresponding to the development of longitudinal cracks in Figure 13 reveals correlation between direction of the vertical movements and the development of longitudinal cracks. According to Figure 13, the maximum percentage of longitudinal cracks occurred between September and November 2017, while the minimum percentage of longitudinal cracks was found between February and April 2018. Exploring the elevation of the road in the above dates indicates that the edge and shoulder points had comparatively low elevations when maximum percentage of longitudinal cracks was observed. On the other hand, comparatively higher elevation was recorded when the percentage of longitudinal cracks was minimum. This observation can be an indication of heaving of the edges of the road at the time the percentage of longitudinal cracks was minimum. To investigate this observation more closely, Figure 16 presents an enlarged presentation of the road surface elevation for the northbound of TS5. This data shows that between November 2017 and April 2018, during which the percentage of longitudinal cracks significantly dropped, the road edge had an upward movement that exceeded 16 mm.

In addition to the evaluation of the transverse section as a whole profile, each point located on the transverse sections can be evaluated separately. For this evaluation, the relative elevation of each point in the first visit was subtracted from the relative elevations obtained in the following visits. Therefore, changes in the elevation of each point on the transverse sections was obtained over time. The center point of each transverse section was referred to as Point 1 and other points were numbered from center to the edge in the order of their distances from the center. An example of this data for the northbound of TS 5 is shown in Figure 17. In general, points near the edge had more fluctuations than points near the center of road. This is consistent with the mechanism introduced by Zornberg et al. (2012) and Roodi et al. (2016) for the development of environmental longitudinal cracks.

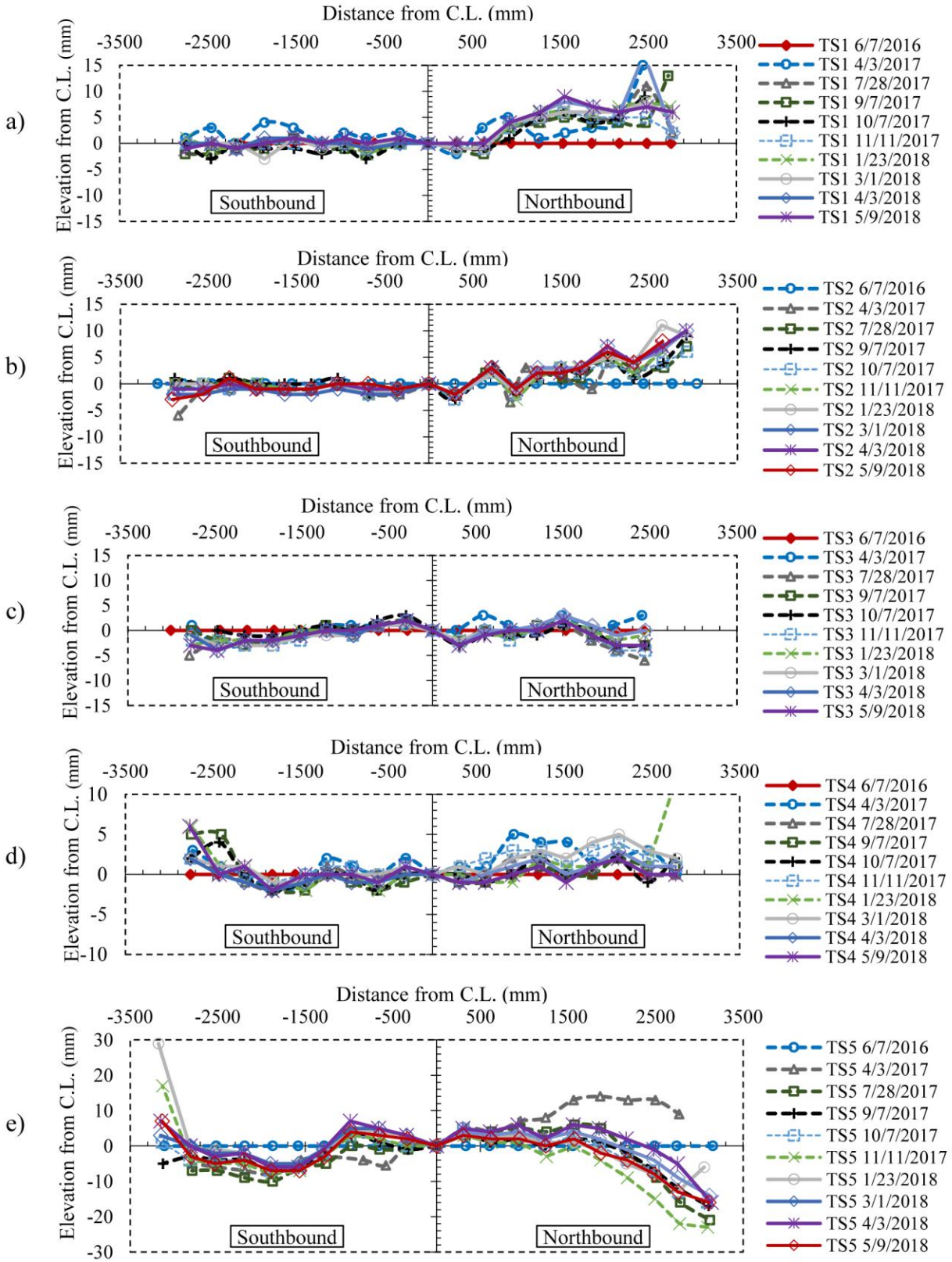

Figure 15. Changes in road surface elevation compared to elevations recorded in the first visit: a) TS1; b) TS2; c) TS3; d) TS4; e) TS5.

Evaluation of the vertical movements presented in Figure 17 between the dates corresponding to the minimum and maximum percentage of longitudinal cracks provides a clear presentation of the previously discussed correlation between the direction of vertical movements and the development of longitudinal cracks. The dates corresponding to the maximum and minimum percentage of longitudinal cracks are highlighted in this figure. A clear rise in the elevation of all points located on this transverse section between the date of maximum crack and the date of minimum crack is observed. Specifically, the magnitude of vertical rise was comparatively larger for points that were located further from the road center (e.g., compare the data for Pts. 9 and 10 with the data for Pts. 4 and 5).

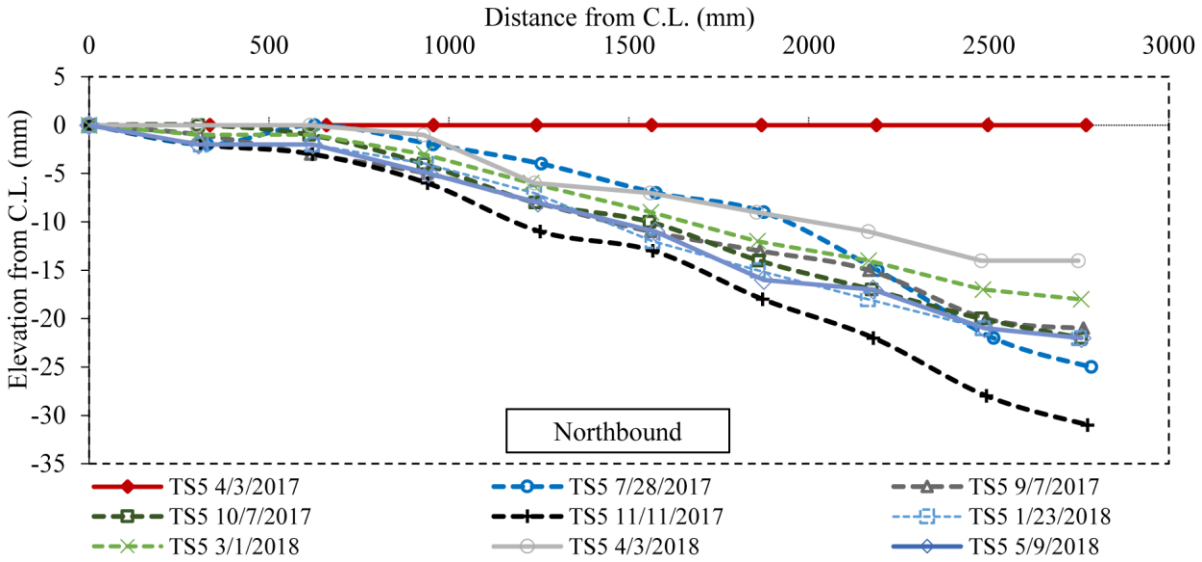

Figure 16. Relative elevation of the road surface the northbound of TS5.

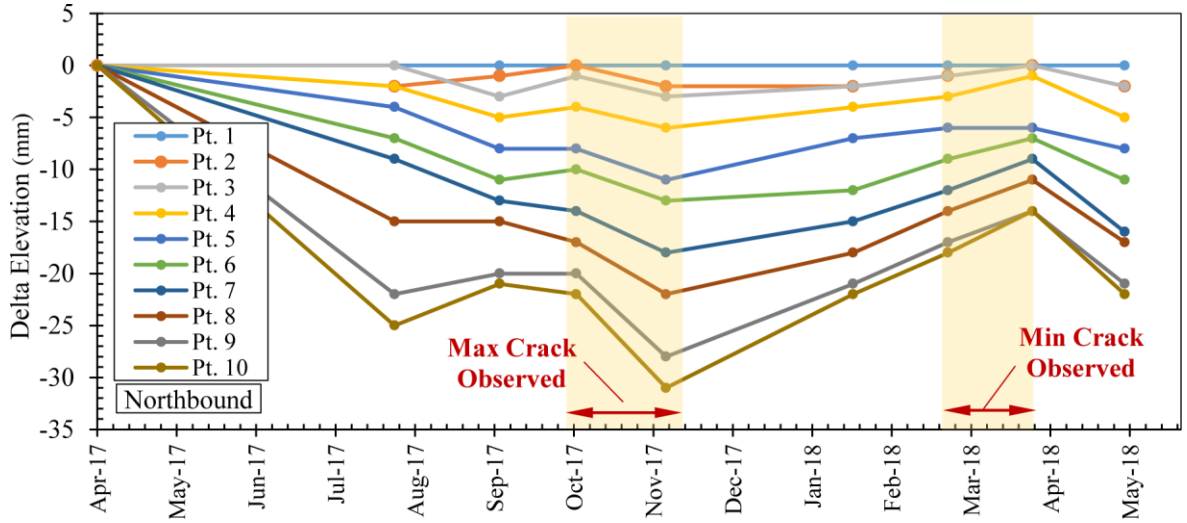

Figure 17. Vertical movements of individual points located on TS5.

Correlation between development of environmental longitudinal cracks and environmental data: In this section, longitudinal cracks were superimposed with environmental data (including cumulative precipitation and temperature data) to evaluate the effect of environmental changes on the development of environmental longitudinal cracks (Figure 18).

The primary vertical axis shows the percentage of longitudinal cracks as well as the temperature in Fahrenheit, and the secondary vertical axis corresponds to the daily precipitation in inches. The maximum percentage of longitudinal cracks was found between September and November 2017. According to the environmental data presented in Figure 18, during the months ending to this period of maximum cracking, the road experienced a relatively dry season coincided with a high temperature. This observation can be seen from the flat portion of the cumulative precipitation data between August and October 2017. In addition, the temperature in these months was particularly high. Starting from October 2017, the temperature drops significantly, which have resulted significant reduction in the moisture loss in the subgrade through evaporation; while at the same time additional relatively steady rainfall provided sources for additional subgrade moisture. Potential increase in the subgrade moisture content under the shoulder resulted in the upward movement of the road edge, which in turn resulted partial closing of longitudinal cracks. Consequently, the percentage of longitudinal cracks significantly reduced after October 2017 and the minimum percentage of longitudinal cracks obtained between February and April 2018.

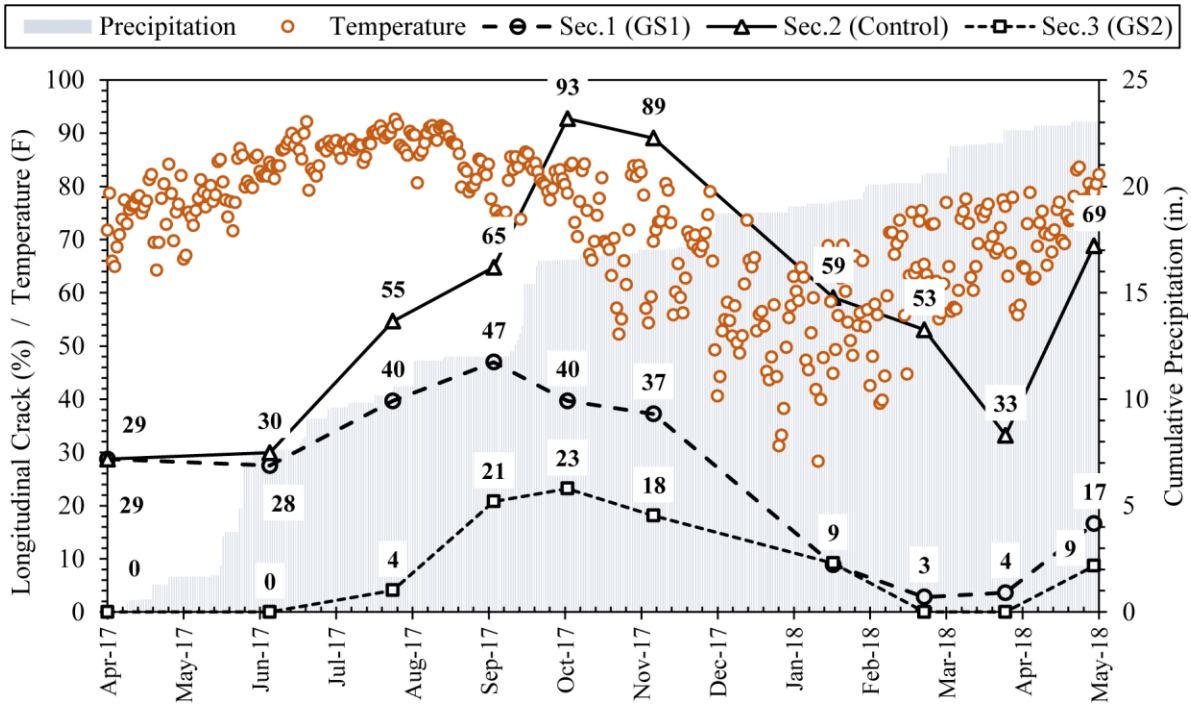

Figure 18. Comparison of longitudinal cracks and environmental data

CONCLUSIONS

Case history of experimental test sections founded over an expansive clay subgrade in Cabeza Road located in Dewitt County, Texas, was presented. The experimental test sections included two sections with geogrid-stabilized flexible base layers, and one control section (non-stabilized flexible base layer). Visual condition surveys and total station surveys were conducted and environmental data were collected over the past three years. Primary findings of this case history are concluded as following:

- The geosynthetic-stabilized sections had significantly lower percentage of environmental longitudinal cracks than the control section.

- The opening and closing of the environmental longitudinal cracks were found to be correlated with the environmental changes at the site. Specifically, temperature and precipitation were found to have key impact on the performance of the test sections. Maximum percentage of the environmental longitudinal cracks was found following a particularly hot and dry season.
- Monitoring vertical movements of several transverse sections of the road using total station revealed seasonal fluctuations of the road surface. Comparison of the vertical movements of the road surface with location of the environmental longitudinal cracks indicated that the southbound of the road that had less vertical movement had also lower percentage of longitudinal cracks as compared to the northbound.
- Geosynthetic stabilization was found not to significantly change the vertical movement of the road. However, it was found that the geosynthetic-stabilized section had significantly lower percentage of longitudinal cracks, as compared to the control section, for similar (or larger) elevation changes. The presence of geogrids could reduce the initiation and development of the environmental longitudinal cracks in the road.
- The vertical movement of the road was found to be comparatively higher near the road edges as compared to the center of the roadway.

ACKNOWLEDGEMENT

The authors wish to thank Texas Department of Transportation and Tensar Co. for their support.

REFERENCES

Chen, D. H. (2007). "Field and lab investigations of prematurely cracking pavements." *Journal of Performance of Constructed Facilities*, Vol. 21, No. 4, pp. 293-301.

Dessouky, S., Oh, J. H., Yang, M., Ilias, M., Lee, S. I., Freeman, T., Bourland, M., and Jao, M. (2012). "Pavement repair strategies for selected distresses in FM roadways." *Texas Department of Transportation, Report No. FHWA/TX-11/0-6589-1*, Austin, TX, USA, 114p.

Weather Underground (2018). "North Runge CR319 KTXRUNGE3, Forecast for Runge, TX." Website.

Roodi, G. H., Phillips, J. R., and Zornberg, J. G. (2016). "Evaluation of Vertical Deflections in Geosynthetic Reinforced Pavements Constructed on Expansive Subgrades." *Proc., 3rd Pan-American Conf. on Geosynthetics, Geo-Americas 2016*, Miami Beach, FL, USA, Vol. 2, pp. 1970 to 1987.

Roodi, G. H., Zornberg, J. G., Aboelwafa, M. M., Phillips, J. R., Zheng, L., and Martinez, J. (2018). "Soil-geosynthetic interaction test to develop specifications for geosynthetic-stabilized roadways." *Rep. No. FHWA/TX-18/5-4829-03-1*, Center for Transportation Research (CTR), Austin, Texas, USA.

USDA (2018). "Web Soil Survey, Soil Map – DeWitt County, Texas." *United States Department of Agriculture*, Website.

Zornberg, J. G., Ferreira, J. A. Z., Gupta, R., Joshi, R. V., and Roodi, G. H. (2012). "Geosynthetic-reinforced unbound base courses: quantification of the reinforcement benefits." *Center for Transportation Research (CTR), Report No. FHWA/TX-10/5-4829-01-1*, Austin, Texas, 170 p.